Energy and angular momentum transfer in the excitation of electron-hole pairs by slow dimers

R. Díez Muiño
Materials Sciences Division, Lawrence Berkeley National Laboratory, Berkeley, California 94720

A. Salin
Laboratoire de Physico-Chimie Moléculaire, UMR 5803 CNRS, Université de Bordeaux I, 351 Cours de la Libération, 33405 Talence Cedex, France

(Received 6 March 2000)

We calculate the transfer of energy and angular momentum through electron-hole pair excitations for a slow dimer in an electron gas. We show that the Kohn-Sham procedure can be used under the adiabatic conditions that prevail in the shifted Fermi sphere approximation. We obtain the low-energy limit of the friction coefficient and average angular momentum transfer from a self-consistent calculation for the embedded dimer. We apply our theory to H_2 and LiH molecules. We use our results to evaluate the role of electron-hole pair excitations when a molecule approaches a metal surface.

I. INTRODUCTION

The study of adsorption and dissociation of molecules on surfaces is a field of great activity due to its implications for catalytic processes. In most cases, the molecule-surface interaction is described by an adiabatic potential-energy surface. The latter approach neglects inelastic processes due to the interaction with phonons and/or electron-hole pair creation. Phonons are of increasing importance when increasing the molecular mass. Many contributions have been devoted to its introduction into molecule-surface dynamics (see, e.g., Refs. 1 and 2 for a review). Much more controversial is the discussion on the contribution of electronic excitations (see Refs. 1 and 3) in spite of experimental evidence.[4,5] The friction caused by electron-hole pair creation is also relevant to energy dissipation by adsorbed species as in vibrational damping[6,7] and electromigration.[8]

Two main families of approaches can be used to evaluate electron-hole pair creation for a moving particle in an electron gas. The first one[7] starts with the conventional Born-Oppenheimer approximation in which the electronic motion is determined in the field of *fixed* nuclei. As electronic excitations of arbitrarily low energy are available in a metal, the motion of the molecule provokes a breakdown of the Born-Oppenheimer approximation. One then follows, as the molecule evolves in the medium, individual electronic excitations giving rise to a frictional and fluctuating force. The second approach, used in the present contribution, makes use of a different adiabatic approximation: the shifted Fermi sphere approximation.[9] It corresponds to a stationary electronic state *in the projectile frame*, which means that the electron gas adapts itself instantaneously to the position of the projectile. However, in contrast with the Born-Oppenheimer approximation, this stationary state accounts for the molecule motion (for example, in the case of a moving atom, the stationary state does not have a spherical symmetry[10]). In this picture, individual electronic excitations are averaged over by the rapid electronic motion (adiabatic approximation) so that the resulting effect is a mere friction force. In other terms, one can view this approximation as corresponding to a ''laminar flow'' of electrons by the projectile, the adiabatic character being related to the absence of ''turbulence.'' This form of the adiabatic approximation should be valid in the low-energy range. It has been used extensively for atoms since the pioneering work of Echenique *et al.*[11] In the low-velocity limit, the stopping power of an electron gas varies linearly with the velocity of the moving particle and can be evaluated from the description of the particle at rest embedded in a jellium.[12] More recently, calculations have been performed[10,13] that go beyond first order in atomic velocity. They have shown that the linear dependence applies up to velocities close to the Fermi velocity. Results for a homogeneous electron gas can be used to evaluate the stopping of atoms or ions approaching a surface through the use of a local approximation.

In the present work we calculate the friction coefficient for a dimer in a homogeneous electron gas. Until now, only preliminary nonlinear calculations have been performed for the molecular case[14–16] because the axial symmetry of the problem complicates the calculation of (i) the static potential of the embedded dimer, and (ii) the scattering of the medium electrons in the latter potential. The first of these two points has been addressed in Ref. 17, where the Kohn-Sham potential has been evaluated self-consistently. We show here that the theory of Ref. 17 provides the ground to calculate the energy loss and angular momentum transfer of slow dimers in a free-electron gas at low velocities. We use the local approximation to estimate the contribution of electronic excitations to the energy dissipation of thermal molecules approaching a metal surface.

Atomic units are used throughout unless otherwise stated.

II. THEORY

A. Kohn-Sham theory for energy and angular momentum transfer

Although Kohn-Sham theory has been used in many nonlinear calculations of the stopping power of an electron gas, to our knowledge no justification of its validity has been proposed. The starting point is a generalization of the proof given in Appendix A of Ref. 10. We introduce the wave function $\Psi(t)$ and Hamiltonian $\hat{H}(t)$ describing the elec-

tronic motion in the presence of the moving projectile (in the present case the dimer). The energy lost by the projectile with velocity $\boldsymbol{v}$ per unit path length is[10]

$$\frac{dE}{dR} = -\frac{1}{v}\langle\Psi(t)|\frac{d\hat{H}(t)}{dt}|\Psi(t)\rangle$$
$$= -\frac{1}{v}\int d\boldsymbol{r}\, n[\boldsymbol{r}-\boldsymbol{R}(t)]\frac{d}{dt}V[\boldsymbol{r}-\boldsymbol{R}(t)]. \quad (1)$$

Here n is the density and V is the interaction potential between the projectile (with position referred to by $\boldsymbol{R}$) and electron. In Eq. (1) we have used the fact that the latter potential is a one-electron local operator. The expression thus obtained depends on the many-electron state only through the density n. It was shown in Ref. 10 that the Kohn-Sham procedure provides the exact time-dependent density in the adiabatic approximation, which is justified for low-projectile velocities. Therefore, Eq. (1) provides the required justification of Kohn-Sham theory for energy-loss calculations in the low velocity limit.

A similar justification of Kohn-Sham theory can be provided for the average angular momentum transfer per unit path length:

$$\frac{d\langle\Delta\hat{\mathbf{J}}\rangle}{dR} = -\frac{1}{v}\frac{d}{dt}\langle\Psi(t)|\hat{\mathbf{J}}|\Psi(t)\rangle = \frac{i}{v}\langle\Psi(t)|[V(t),\hat{\mathbf{J}}]|\Psi(t)\rangle. \quad (2)$$

The operator $\hat{\mathbf{J}}$ is a one-electron and first-order differential operator. Therefore, Eq. (2) can also be cast into a form similar to that of Eq. (1), i.e., depending on the many-electron state through the density only. This justifies again the use of Kohn-Sham theory.

Once we have shown the validity of the Kohn-Sham procedure, we are then led to solving a much simpler problem in which the projectile interacts with noninteracting electrons. Within Kohn-Sham theory, it is equivalent to calculate the energy loss through Eq. (1) or through the energy transfer by electron scattering in the Kohn-Sham potential of the moving dimer (see, e.g., Ref. 10). A similar equivalence holds for the evaluation of the angular momentum transfer.

In practice, the static Kohn-Sham potential has been determined within the local-density approximation (LDA). The relevant methods have been described elsewhere[17] and are only summarized here. We expand the external and total potentials, as well as the electronic density induced by the dimer in the medium, in terms of Legendre polynomials. A partial-wave expansion is used for the Kohn-Sham orbitals. Consequently, the usual Kohn-Sham equations are transformed into a system of coupled equations for each value of the energy and the magnetic quantum number m. The system of coupled equations is solved after truncation of the partial-wave expansion and potential multipolar expansion at certain maximum values ($l_{\max}$ and $\nu_{\max}$, respectively).

B. Energy transfer

Our starting point is the expression of the energy transfer for a projectile of mass much larger than the electron mass. To first order in the ratio of the electron to projectile mass, the energy transfer may be associated with the momentum transfer to the electrons $\Delta\boldsymbol{k}$ through the expression

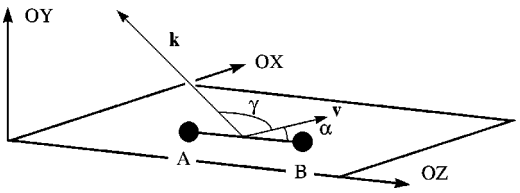

FIG. 1. Geometry and notations. The dimer axis is along OZ and the velocity $\boldsymbol{v}$ lies in the XZ plane. We name α the polar angle of $\boldsymbol{v}$ with respect to OZ and γ the angle between $\boldsymbol{k}$ and $\boldsymbol{v}$.

$$\Delta E = \boldsymbol{v}\cdot\Delta\boldsymbol{k}. \quad (3)$$

Let $\boldsymbol{k}$ and $\boldsymbol{k}'$ $(k=k')$ be the initial and final momenta of the electron in an individual collision. The total energy lost by the projectile per unit path length S is:

$$S = \frac{dE}{dR} = \frac{1}{4\pi^3}\int_{\mathrm{SFS}} d^3\boldsymbol{k}k^2\hat{\boldsymbol{v}}\cdot\boldsymbol{\sigma}_{\mathrm{tr}}(\boldsymbol{k}), \quad (4)$$

where $\hat{\boldsymbol{v}}$ is a unitary vector along the direction of the velocity and the integration is performed over a shifted Fermi sphere (SFS). As the Kohn-Sham potential does not have a spherical symmetry for the dimer case, the transport cross section $\boldsymbol{\sigma}_{\mathrm{tr}}(\boldsymbol{k})$ is a vector quantity:

$$\boldsymbol{\sigma}_{\mathrm{tr}}(\boldsymbol{k}) = \int d\Omega_{\mathbf{k}'}(\hat{\boldsymbol{k}}-\hat{\boldsymbol{k}}')|f(\boldsymbol{k},\boldsymbol{k}')|^2. \quad (5)$$

Here $\hat{\boldsymbol{k}}$ and $\hat{\boldsymbol{k}}'$ are unitary vectors in the $\boldsymbol{k}$ and $\boldsymbol{k}'$ directions respectively, and $f(\boldsymbol{k},\boldsymbol{k}')$ is the transition amplitude from initial state $\boldsymbol{k}$ to final state $\boldsymbol{k}'$. The transition amplitude is obtained from

$$f(\boldsymbol{k},\boldsymbol{k}') = \frac{2\pi}{ik}\sum_{l,m} A_{lm}(\boldsymbol{k})Y_l^m(\Omega_{\mathbf{k}'}), \quad (6)$$

with

$$A_{lm}(\boldsymbol{k}) = \sum_{l',m} t_{ll'}^m(k)[Y_{l'}^m(\Omega_{\mathbf{k}})]^*,$$
$$t_{ll'}^m(k) = i^{l'-l}S_{ll'}^m(k) - \delta_{ll'}, \quad (7)$$

and $Y_l^m(\Omega_{\mathrm{k}'})$ are spherical harmonics. The scattering matrices $S_{ll'}^m(k)$ are built using the asymptotic behavior of the Kohn-Sham orbitals.[10,17] For a spherically symmetric potential, $S_{ll'}^m(k)$ is a diagonal matrix with elements $e^{2i\delta_l}$, δ_l being the phase shifts, and the conventional expression is regained.

For the evaluation of Eq. (4), we use the geometry depicted in Fig. 1. The OZ axis is the dimer axis and points from atom A towards atom B. The velocity lies in the XZ plane. The angle between the velocity and the dimer axis is α and the angle between the velocity and the $\boldsymbol{k}$ vector is γ. The integral in Eq. (4) is easily performed to first order in the velocity to obtain

$$S \rightarrow_{v\to 0} \frac{1}{4\pi^3}\int d\Omega_{\mathbf{k}_F}(1-\cos\gamma)k_F^4\boldsymbol{v}\cdot\boldsymbol{\sigma}_{\mathrm{tr}}(\boldsymbol{k}_F), \quad (8)$$

in which the transport cross section is calculated for a static dimer. The expression for a spherically symmetric potential

can be easily recovered for cross-checking purposes: then $\boldsymbol{\sigma}_{\rm tr}(\boldsymbol{k}_F)$ is a scalar quantity that only depends on the cosine of the angle between $\boldsymbol{k}$ and $\boldsymbol{k}'$.

It is important to realize that a consistent calculation to first order in the velocity using the static Kohn-Sham potential requires Eq. (8). It has been shown[10] already that the direct use of Eq. (1) with a density determined from the static potential leads to incorrect results. This can be verified for the case of Ref. 6: we have checked that the error shown in Table III of the latter reference is almost totally explained by the use of the incorrect procedure.

The first term inside the integral in Eq. (8) gives a zero contribution since[18]

$$f(\boldsymbol{k},\boldsymbol{k}')=f(-\boldsymbol{k}',-\boldsymbol{k}). \tag{9}$$

If we decompose the transport cross section into components parallel and perpendicular to the dimer axis, the energy loss can be written as

$$S(\alpha)=F_{\parallel}v\cos^2\alpha+F_{\perp}v\sin^2\alpha, \tag{10}$$

with

$$F_{\parallel}=-\frac{k_F^4}{4\pi^3}\int d\Omega_{\mathbf{k}_F}\sigma_{\rm tr}^{\parallel}(\boldsymbol{k}_F)\cos\theta_{\mathbf{u}_F} \tag{11}$$

and

$$F_{\perp}=-\frac{k_F^4}{4\pi^3}\int d\Omega_{\mathbf{k}_F}\sigma_{\rm tr}^{\perp}(\boldsymbol{k}_F)\sin\theta_{\mathbf{k}_F}\cos\varphi_{\mathbf{u}_F}. \tag{12}$$

$F_{\parallel}$ and $F_{\perp}$ represent the friction coefficient (i.e., the stopping power per unit of velocity) of a dimer moving along a direction parallel or perpendicular to its axis. Due to the axial symmetry of the problem, $F_{\perp}$ accounts for the friction coefficient in both the OX and OY directions. For any other orientation of the dimer, the stopping power is a combination of the $F_{\parallel}$ and $F_{\perp}$ components through Eq. (10). The latter expression shows that the energy lost by an asymmetric dimer is identical for $\alpha=0$ and $\alpha=\pi$ to first order in v. However, the linear momentum transferred by one electron in a single collision is different (if the molecule is asymmetric) when the incident angle of the incoming electron is $\theta_{\mathbf{k}}=0$ and when it is $\theta_{\rm k}=\pi$. The identity $S(0)=S(\pi)$ only appears after performing the integral over the whole range of initial and final angles, and is a consequence of the symmetry properties of the transition amplitude [Eq. (9)].

In order to obtain the parallel and perpendicular components of S, let us calculate first $\sigma_{\rm tr}^{\parallel}$ and $\sigma_{\rm tr}^{\perp}$:

$$\begin{aligned}\sigma_{\rm tr}^{\parallel}(\boldsymbol{k})&=\int d\Omega_{\mathbf{k}'}(\cos\theta_{\boldsymbol{k}}-\cos\theta_{\mathbf{k}'})|f(\boldsymbol{k},\boldsymbol{k}')|^2\\&=\frac{4\pi^2}{k^2}\sum_{l,m}\left(|A_{lm}(\boldsymbol{k})|^2\cos\theta_{\mathbf{k}}-\frac{1}{\sqrt{3}}\right.\\&\left.\times\sum_{l'}A_{lm}^{*}(\boldsymbol{k})A_{l'm}(\boldsymbol{k})\zeta(l,l',1;m,m,0)\right),\end{aligned} \tag{13}$$

$$\begin{aligned}\sigma_{\rm tr}^{\perp}(\boldsymbol{k})&=\int d\Omega_{\mathbf{k}'}(\sin\theta_{\mathbf{k}}\cos\varphi_{\mathbf{k}}-\sin\theta_{\mathbf{k}'}\cos\varphi_{\mathbf{k}'})|f(\boldsymbol{k},\boldsymbol{k}')|^2\\&=\frac{4\pi^2}{k^2}\left\{\sum_{l,m}|A_{lm}(\boldsymbol{k})|^2\sin\theta_{\mathbf{k}}\cos\varphi_{\boldsymbol{k}}-\sqrt{\frac{2}{3}}\right.\\&\times\sum_{l,l',m}\mathrm{Re}[A_{lm}^{*}(\boldsymbol{k})A_{l'm+1}(\boldsymbol{k})\\&\left.\times\zeta(l,l',1;m,m+1,-1)]\right\},\end{aligned} \tag{14}$$

where Re stands for real part and the angular $\zeta(l_1,l_2,l_3;m_1,m_2,m_3)$ coefficients are the result of composing three spherical harmonics, and are defined in terms of Wigner $3j$ symbols:

$$\begin{aligned}&\zeta(l_1,l_2,l_3;m_1,m_2,m_3)\\&=(-1)^{m_1}(2l_1+1)^{1/2}(2l_2+1)^{1/2}(2l_3+1)^{1/2}\\&\times\begin{pmatrix}l_1&l_2&l_3\\0&0&0\end{pmatrix}\begin{pmatrix}l_1&l_2&l_3\\-m_1&m_2&m_3\end{pmatrix}.\end{aligned} \tag{15}$$

The sums over l in Eqs. (13) and (14) run from $l=0$ to $l=l_{\max}$. The allowed values of l' and m are determined by the properties of the angular coefficients ζ. This is also true for the sums appearing in the following equations and for which the limits are not explicitly written. Introducing these expressions in Eqs. (11) and (12) and performing the angular integration, we obtain

$$\begin{aligned}F_{\parallel}=-\frac{k_F^2}{3\pi}\sum_{l,l_1,m}&\left\{|t_{ll_1}^{m}|^2+\frac{2}{\sqrt{5}}\sum_{l_2}\zeta(l_1,l_2,2;m,m,0)\right.\\&\times(t_{ll_1}^{m})^{*}t_{ll_2}^{m}-\sum_{l_3}\sum_{l_4}\zeta(l,l_4,1;m,m,0)\\&\left.\times\zeta(l_1,l_3,1;m,m,0)(t_{ll_1}^{m})^{*}t_{l_4l_3}^{m}\right\},\end{aligned} \tag{16}$$

$$\begin{aligned}F_{\perp}=-\frac{k_F^2}{3\pi}\sum_{l,l_1,m}&\left\{|t_{ll_1}^{m}|^2-\frac{1}{\sqrt{5}}\sum_{l_2}\zeta(l_1,l_2,2;m,m,0)\right.\\&\times(t_{ll_1}^{m})^{*}t_{ll_2}^{m}-\mathrm{Re}\left(\sum_{l_3}\sum_{l_4}\zeta(l,l_4,1,m,m+1,-1)\right.\\&\left.\left.\times\zeta(l_1,l_3,1;m,m+1,-1)(t_{ll_1}^{m})^{*}t_{l_4l_3}^{m+1}\right)\right\}.\end{aligned} \tag{17}$$

Notice that the calculation of the perpendicular friction coefficient involves the coupling of terms with different m symmetry. Up to this point, the formalism developed for the calculation of $F_{\parallel}$ and $F_{\perp}$ is general and exact. It only requires the knowledge of the scattering amplitude $f(\boldsymbol{k},\boldsymbol{k}')$ (or, equivalently, of the scattering matrix elements $t_{ll'}^{m}$ from which the scattering amplitude is obtained) for a given potential of axial symmetry.

One keypoint in the energy lost per unit path length S is the linear dependence on the velocity. As the kinetic energy E of the projectile is proportional to the square of the velocity, the relative energy loss scales with the inverse of the velocity:

$$\frac{S}{E} \propto_{v\to 0} \frac{1}{v} \tag{18}$$

[the latter expression holds as long as Eq. (3) is valid, which is not the case for extremely low energies]. In other words, the relative importance of the energy lost by the particle through excitations of electron-hole pairs is enhanced for small velocities and will be especially important in the range of thermal energies.

C. Angular momentum transfer

As for the calculation of energy transfer, the Kohn-Sham formalism allows us to calculate angular momentum transfer from the angular momentum change of the electrons when scattered by the dimer. The equivalent of Eq. (4) for the average angular momentum transfer $\langle \Delta \hat{\mathbf{J}} \rangle$ per unit path length is

$$\frac{d\langle \Delta \hat{\mathbf{J}} \rangle}{dR} = -\frac{1}{4\pi^3 v} \int_{\mathrm{SFS}} d^3\boldsymbol{k} k \sigma_{\Delta \hat{\mathbf{J}}}(\boldsymbol{k}), \tag{19}$$

where $\sigma_{\Delta \hat{\mathbf{J}}}(\boldsymbol{k})$ is the angular momentum transfer cross section. The latter measures the average change of $\Delta \hat{\mathbf{J}}$ for electrons with momentum $\boldsymbol{k}$ scattered by the projectile. Using considerations similar to those of the preceding paragraph, one obtains the low-velocity limit of the average angular momentum transfer per unit path length:

$$\frac{d\langle \Delta \hat{\mathbf{J}} \rangle}{dR} \to_{v\to 0} -\frac{k_F^3}{4\pi^3} \int d\Omega_{\mathbf{u}_F} (1-\cos\gamma) \sigma_{\Delta \hat{\mathbf{J}}}(\boldsymbol{k}_F), \tag{20}$$

where $\sigma_{\Delta \hat{\mathbf{J}}}(\boldsymbol{k})$ is now calculated for a static dimer. Therefore, the angular momentum change (20) is independent of the velocity. To evaluate the angular momentum transfer cross section, we make use of the density operator formalism.[19] As continuum wave functions are not normalizable, we use a generalization of the latter formalism which accounts for the fact that we only carry out angular averages outside the range of the potential. Then, the density operator $\hat{\rho}$ for the scattered electrons may be written in the $|\hat{\boldsymbol{k}}\rangle$ representation as

$$\hat{\rho} = C \int d\hat{\boldsymbol{k}}' \int d\hat{\boldsymbol{k}}'' F(\boldsymbol{k},\boldsymbol{k}') |\hat{\boldsymbol{k}}'\rangle\langle \hat{\boldsymbol{k}}''| F^*(\boldsymbol{k},\boldsymbol{k}''),$$
$$F(\boldsymbol{k},\boldsymbol{k}') = f(\boldsymbol{k},\boldsymbol{k}') + \frac{2\pi}{ik} \delta(\hat{\boldsymbol{k}}' - \hat{\boldsymbol{k}}), \tag{21}$$

where C is a normalization constant. We name $\hat{\rho}_0 = (4\pi^2 C/k^2) |\hat{\boldsymbol{k}}\rangle\langle \hat{\boldsymbol{k}}|$ the density operator in the absence of a potential. The average change, due to the potential, in the mean value of an observable $\hat{O}$ is

$$\begin{aligned}\langle \Delta \hat{O} \rangle &= \mathrm{Tr}[\hat{\rho}\hat{O} - \hat{\rho}_0 \hat{O}] \\ &= C \int d\hat{\boldsymbol{k}}' d\hat{\boldsymbol{k}}'' f(\boldsymbol{k},\boldsymbol{k}') f^*(\boldsymbol{k},\boldsymbol{k}'') \langle \hat{\boldsymbol{k}}''| \hat{O} |\hat{\boldsymbol{k}}'\rangle \\ &\quad - C \frac{4\pi}{k} \int d\hat{\boldsymbol{k}}' \, \mathrm{Im}[\langle \hat{\boldsymbol{k}}| \hat{O} |\hat{\boldsymbol{k}}'\rangle f(\boldsymbol{k},\boldsymbol{k}')],\end{aligned} \tag{22}$$

where Tr stands for the trace and Im for the imaginary part. The constant C may be determined by calculating the change in the average momentum (the observable $\hat{O}$ being then the momentum operator) and using Eq. (5). One gets $C = [\sigma_T(\boldsymbol{k})]^{-1}$ with

$$\sigma_T(\boldsymbol{k}) = \int d\Omega_{\mathbf{k}'} |f(\boldsymbol{k},\boldsymbol{k}')|^2. \tag{23}$$

Switching to the $|l,m\rangle$ representation, one gets the expression of the angular momentum transfer cross section:

$$\begin{aligned}\sigma_{\Delta \hat{\mathbf{J}}}(\boldsymbol{k}) &= \sigma_T(\boldsymbol{k}) \langle \Delta \hat{\mathbf{J}} \rangle \\ &= \frac{4\pi^2}{k^2} \Bigg\{ \sum_{l,m} \sum_{l'm'} A_{lm}(\boldsymbol{k}) A^*_{l'm'}(\boldsymbol{k}) \langle l',m'| \hat{\mathbf{J}} |l,m\rangle \\ &\quad - 2 \sum_{l,m} \sum_{l'm'} \mathrm{Im}[\langle \hat{\boldsymbol{k}}| l',m'\rangle \langle l',m'| \hat{\mathbf{J}} |l,m\rangle A_{l,m}(\boldsymbol{k})] \Bigg\}.\end{aligned} \tag{24}$$

Due to the symmetry of the problem (see Fig. 1) only the $\hat{J}_y$ component of the vector operator $\hat{\mathbf{J}}$ gives a nonzero contribution after averaging over angles as in Eq. (19). This can be checked analytically through Eq. (24) after some elementary algebra. The final result may be obtained from Eqs. (20) and (24):

$$\begin{aligned}\frac{d\langle \Delta \hat{J}_y \rangle}{dR} &= \sqrt{\frac{1}{6\pi^2}} k_F \sin\alpha \sum_{l,l'} \sum_{m} [l(l+1) - m(m+1)]^{1/2} \\ &\quad \times \mathrm{Im} \Bigg\{ \sum_{l''} \zeta(l',l'',1;m,m+1,-1) t^m_{l,l'} (t^{m+1}_{l,l''})^* \\ &\quad + 2\zeta(l',l,1;m+1,m,1) t^{m+1}_{l,l'} \Bigg\},\end{aligned} \tag{25}$$

where the sums over l', l'', and m are restricted by the values of the angular ζ coefficients. The dependence on $(\sin\alpha)$ in Eq. (25) ensures the absence of angular momentum transfer when the molecule moves along a direction parallel to its axis.

For the sake of simplicity, we will denote in the following

$$\Lambda = \frac{1}{\sin\alpha} \frac{d\langle \Delta \hat{J}_y \rangle}{dR}. \tag{26}$$

D. Independent-atom approximation

Former theoretical studies of the energy loss of a dimer inside a free-electron gas made use of the independent-atom (IA) approximation. In this work, we will use it as a check of our calculations in some limit cases. In the IA approximation, one assumes that the atoms travel independently

through the electron gas. First, this means that the Kohn-Sham potential may be split into two nonoverlapping parts ($V=V_A+V_B$) where the potentials $V_{A,B}$ are those of isolated atoms embedded in the electron gas. Second, the transition amplitude is calculated through the expression[20]

$$f_{\mathrm{IA}}(\boldsymbol{k},\boldsymbol{k}')=e^{-ikd(\cos\theta_{\mathbf{k}}-\cos\theta_{\mathbf{k}'})/2}f_A(\boldsymbol{k},\boldsymbol{k}') + e^{ikd(\cos\theta_{\mathbf{k}}-\cos\theta_{\mathbf{k}'})/2}f_B(\boldsymbol{k},\boldsymbol{k}'), \qquad (27)$$

where $f_{A,B}$ is the scattering amplitude for the potential $V_{A,B}$ alone. Multiple scattering events of the electron in the two potentials are thus neglected. Equation (27) is valid when $kd\gg 1$. In the IA approximation, the only effect due to the simultaneous presence of two atoms is the interference embedded in Eq. (27). The IA approximation is accurate in certain limits, the most obvious one being that of large internuclear distances d. It is also exact in the perturbative limit because of the linear dependence of the scattering amplitude on the potential.

III. ENERGY LOSS

We first consider the energy loss of H_2 in a free-electron gas (FEG). This problem has already a long history because of its relation with measurements of the so-called *vicinage effect*. The vicinage effect has been observed experimentally as a difference between the energy loss of two protons and that of a dimer.[21,22] Until recently, all calculations on the vicinage effect were done in the IA approximation. Early contributions by Basbas and Ritchie[23] were based on linear-response theory. More recently, the IA approximation has been used together with a nonlinear evaluation of the medium response (i.e., using the atomic Kohn-Sham potentials for the evaluation of $f_{A,B}$) to study the stopping of H_2^+ molecular ions.[15]

The only previous contribution going beyond the IA approximation is that of Urbassek *et al.*,[16] which focused on the H_2^+ ion as well. The latter authors calculate exactly the scattering amplitude for a two-center potential. However, the form of their potential is restricted by the method used in the solution of the scattering problem. In particular, it does not go to the correct limit for increasing d. Furthermore, this potential is determined *a priori*. In the present work, we determine the two-center potential self-consistently and the scattering on this potential is evaluated exactly.

Our calculations have been done with typical values $\nu_{\max}=$ 8–10 and $l_{\max}=10$–12 (Ref. 17). In Fig. 2 we show the friction coefficients $F_\parallel$ and $F_\perp$ for H_2 in a FEG as a function of r_s ($1/n_o=4\pi r_s^3/3$) over the range of metallic electronic densities. The internuclear distance between the two nuclei is kept fixed at the H_2 equilibrium distance in vacuum ($d_{\mathrm{eq}}=1.4$ a.u.). The difference between $F_\parallel$ and $F_\perp$ is significant. For the highest densities shown in the plot, $F_\perp$ is twice as large as $F_\parallel$, while $F_\parallel>F_\perp$ for $r_s>3.2$. The orientation effect cannot be explained by simple terms. Scattering by the two-center potential is a complex process[16] depending both on Fermi energy and internuclear distance which precludes any simple prediction of the orientation effect. It is related essentially to interference effects in two-center scattering since one has also $F_\perp>F_\parallel$ for the IA approximation at the equilibrium distance.

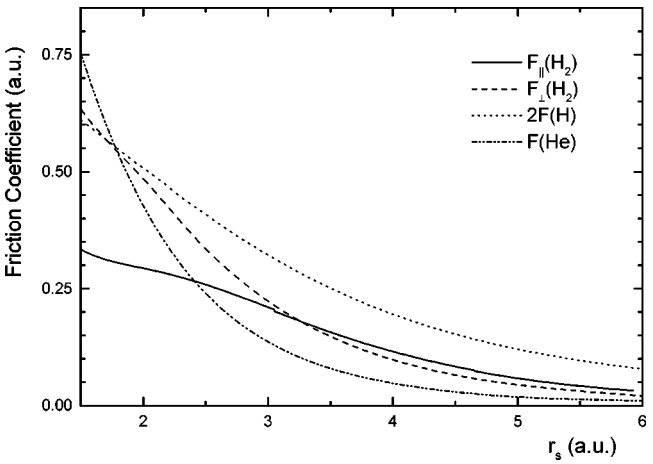

FIG. 2. Friction coefficients (stopping power per unit of velocity) for H_2 as a function of electronic density parameter r_s. Solid line: H_2 moving parallel to its axis ($F_\parallel$). Dashed line: H_2 moving perpendicular to its axis ($F_\perp$). Dotted line: twice the friction coefficient of H. Dash-dotted line: results for He.

We also plot in Fig. 2 the friction coefficient for He and twice that of H, which corresponds to the limits $d=0$ and $d=\infty$, respectively. For increasing r_s, the Fermi wavelength increases and the two-center character of the potential is not so important. Accordingly, the dimer friction gets closer to that of He. For large densities, the opposite situation would hold and the dimer friction would go to twice that of H. The orientation effect is therefore at maximum for $k_F d\sim 1$, which corresponds to metallic densities ($r_s=1.4$ for $k_F d=1$).

In Fig. 3, we plot the friction coefficients for H_2 as a function of the internuclear distance d and for various electron-gas densities. The zero internuclear distance limit agrees (as it should) with the energy loss of the He atom. For large distances, $F_\parallel$ and $F_\perp$ should merge to twice the stopping of a H atom. The latter value is indicated by small arrows on the right side of Fig. 3. For $d=7$ a.u. the asymptotic limit is still not reached, the difference being larger for small electronic densities, as expected from condition $k_F d\gg 1$ for the validity of the IA approximation.

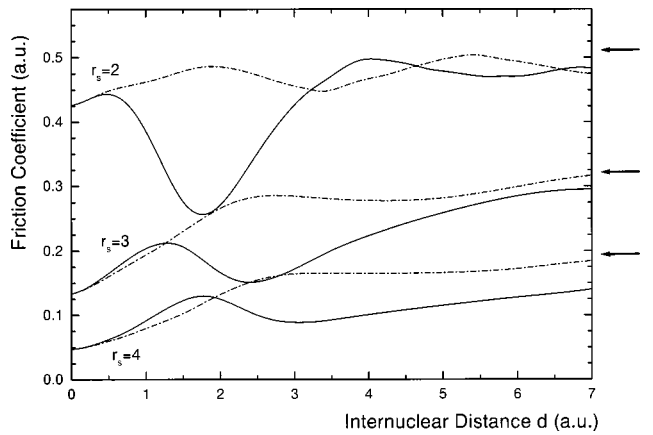

FIG. 3. Parallel ($F_\parallel$, solid line) and perpendicular ($F_\perp$, dash-dotted line) friction coefficients for H_2 in a free electron gas as a function of internuclear distance d and for $r_s=2,3,4$. The arrows at the right side of the plot represent twice the friction coefficient for H.

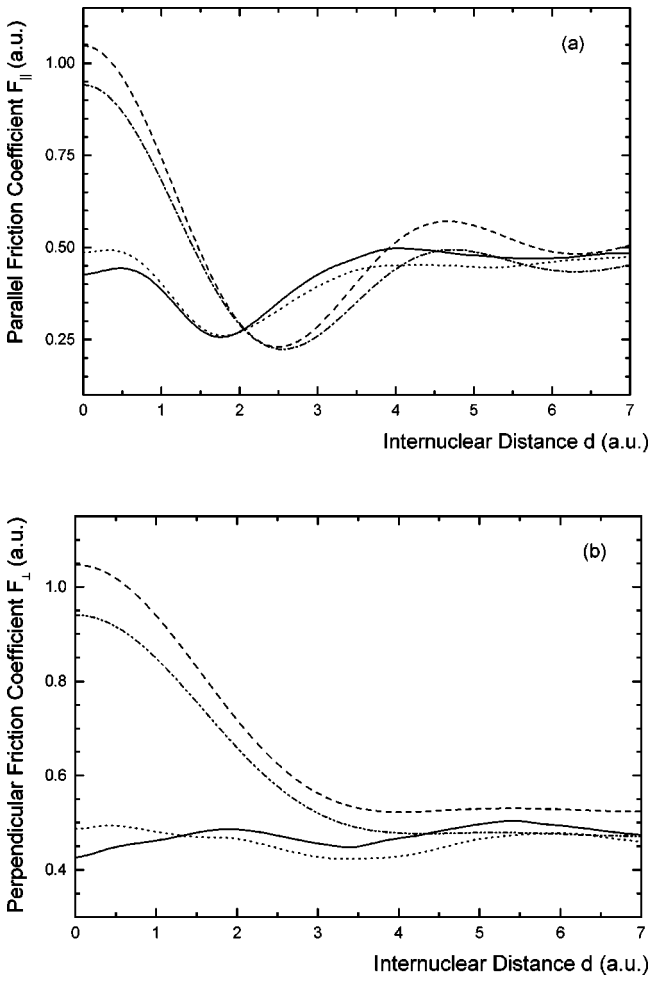

FIG. 4. Friction coefficients for a H_2 molecule moving parallel (a) and perpendicular (b) to its axis in a free-electron gas of $r_s=2$ as a function of internuclear distance d. Results of four different calculations are plotted: (i) IA approximation with Yukawa atomic potentials (dash-dotted line), (ii) IA approximation with Kohn-Sham atomic potentials (dashed line), (iii) two-center calculation for a superposition of two Yukawa potentials (dotted line), (iv) calculation for the dimer Kohn-Sham potential (solid line).

The most obvious feature of Fig. 3 is the oscillation of the friction coefficient as a function of d. The period of the oscillations is different for $F_\parallel$ and $F_\perp$. $F_\parallel$ has a deep minimum that moves towards larger distances as r_s increases. These oscillations are related to an interference effect for scattering on the two-center potential of the same nature as the one found in the IA expression (27). This interference affects in a different way the perpendicular and parallel cross sections and, therefore, the oscillation period is different for $\sigma_{\rm tr}^{\parallel}$ and $\sigma_{\rm tr}^{\perp}$.

Our results include nonlinear effects both in the medium response to the dimer potential and in the calculation of the scattering amplitude. Consequently, they can be taken as a reference to check the accuracy of other approximations used in the literature. In Fig. 4, we give results for $F_\parallel$ and $F_\perp$ as a function of the internuclear distance using four different models. Two of the calculations are done within the IA approximation: (i) with a Yukawa potential with Thomas-Fermi screening and (ii) with the self-consistent potential for an embedded atom. The other two calculations make use of a two-center potential. One of them (iii) is the sum of two Yukawa potentials

$$V(\boldsymbol{r})=\frac{e^{-\lambda|\mathbf{r}-\mathbf{d}/2|}}{|\boldsymbol{r}-\boldsymbol{d}/2|}+\frac{e^{-\lambda|\mathbf{r}+\mathbf{d}/2|}}{|\boldsymbol{r}+\boldsymbol{d}/2|} \tag{28}$$

(where λ is the Thomas-Fermi screeening constant) and the other (iv) is our self-consistent potential for the embedded H_2 molecule. The Yukawa potential corresponds to a linear description of the screening around each nucleus of the dimer.

Calculation (ii) is equivalent to that of Ref. 15 (except that only the $l=0$ phase shift was included in the latter). Calculation (iii) slightly improves that of Ref. 16. As can be seen in Fig. 4, calculations (i) and (ii) or (iii) and (iv) do not differ considerably. However, there is a large discrepancy between calculations performed with the full two-center potential [(iii) and (iv)] and those using the IA [(i) and (ii)]. The IA approximation, therefore, breaks down completely in the most important range of d values. The use of a two-center potential (rather than the IA approximation) is much more important than the particular form of potential used in the calculation. It should be noted that when we use Yukawa potentials arising from a linear theory of screening, we perform exact nonlinear calculations of the scattering amplitude. The error involved in using linear theory for the amplitudes also (first Born approximation) is large, as already demonstrated for embedded atoms, which gives information on the $d=0$ limit of our calculations.

We have used our results to estimate the energy lost through electron-hole pair excitation by a H_2 molecule with thermal translation energy E_i approaching a metal surface. To do so, we describe the electronic density of the surface by a density profile $n(z)$, where z is the distance to the surface. The energy loss at a given distance z from the surface is approximated by the energy that would lose the molecule in a jellium with electronic density $n(z)$ (*local approximation*). The energy lost by the molecule up to a distance z_0 from the surface can be calculated by

$$\epsilon(z_o)=\int_{\infty}^{z_0} dz\, S[\alpha,n(z)], \tag{29}$$

where α is the angle between the axis of the molecule and the velocity. Although a rough approximation, the local approximation should give at least an order of magnitude estimate. We use two different descriptions of the surface electronic density profile: (i) a phenomenological one, in which $n(z)=n_0 e^{-\sqrt{2\phi}z}$, where n_0 is the bulk valence-band electronic density and ϕ is the experimental work function; (ii) the DFT electronic density profile calculated by Lang and Kohn.[24] In this description, z represents the distance to the jellium edge. We have chosen Al as a test case, because Al is a free-electron-like metal. We plot in Fig. 5 the relative energy loss $\epsilon(z_0)/E_i$ for a molecule approaching the surface along the surface normal for two different molecular orientations (parallel and perpendicular to the surface). Furthermore, we plot in Fig. 5 twice the relative energy loss of a H atom approaching the surface. The results are fairly sensitive to the choice of density profile. In the following, we only discuss Fig. 5(b), which we consider more realistic. Several

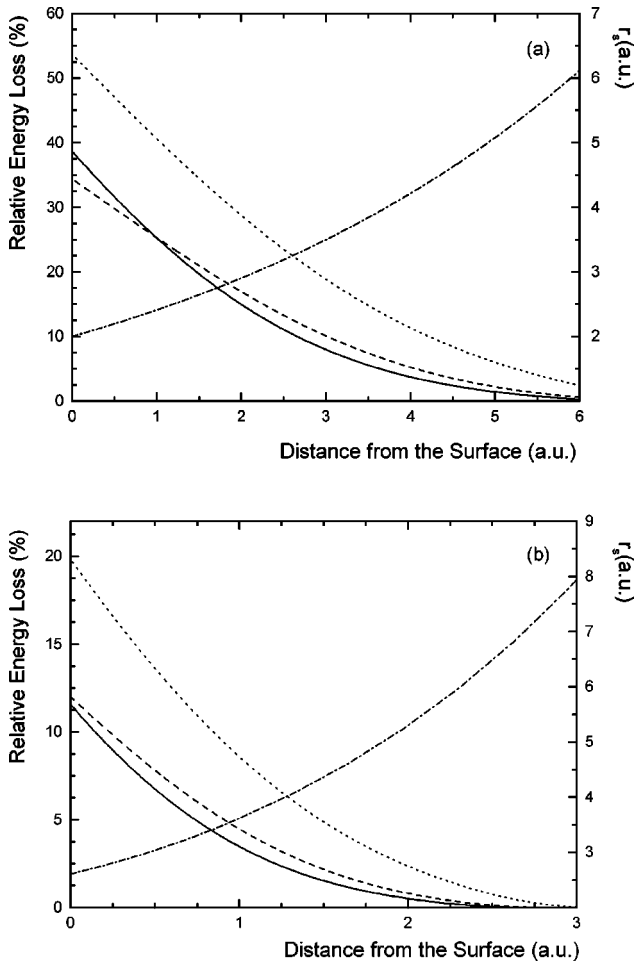

FIG. 5. Relative energy loss $[\epsilon(z_0)/E_i]$ for a H_2 molecule approaching an Al surface. The molecule is incident perpendicular to the surface with energy $E_i=100$ meV. The molecular axis is parallel (solid line) or perpendicular (dashed line) to the surface. The dotted line corresponds to twice the results for H. The right axis refers to the value of the electronic density parameter r_s (dash-dotted line) as a function of the distance to the surface. (a) Density profile $n(z)=n_0e^{-\sqrt{2\phi}z}$; (b) density profile of Lang and Kohn. (Ref. 24).

conclusions can be extracted from the plot, namely, (i) the energy loss has a slight dependence on the molecule orientation, (ii) the relative energy loss can be as much as 10% for $E_i=100$ meV, and (iii) the vicinage effect causes an important reduction of the energy loss. It is important to notice at this point that the value of the energy loss plotted in Fig. 5 is a lower limit: When the adsorption of H_2 is dissociative, the energy lost by excitation of electron-hole pairs through the dissociative adsorption process should be somewhere in between results for the equilibrium distance and those for d infinite, thus increasing its value. Furthermore, if the incident angle of the impinging molecule deviates from the surface normal, the path length over which the molecule interacts with the surface electronic density is larger and, subsequently, the energy lost by the molecule is enhanced.

The present results are relevant to the extraction of activation barriers from experimental threshold positions. When the experimental threshold is of the order of 0.1 eV, we have to take into account the fact that the slowing down of the molecule induces a shift in the threshold apparent position by 10–20 % at least toward larger energies. In fact, the error is certainly larger since the barrier slows down the molecule with a correlative increase in the relative energy loss [cf. Eq. (18)]. Another situation for which the error will be significant is in using microreversibility to calculate adsorption probabilities from desorption ones.[25]

IV. ANGULAR MOMENTUM TRANSFER

Our evaluation of the angular momentum transfer to the nuclei assumes that the molecule has a fixed internuclear distance. The problem is more involved if vibrational motion is taken into account. A more accurate evaluation would require us to work out the full molecular dynamics.

The quantity obtained in Sec. II C is the angular momentum lost by the electrons. The angular momentum transferred to the molecule must be equal in absolute value and opposite in sign, due to the angular momentum conservation law. The results that we present in this section are calculated in the reference frame used for the determination of the electronic wave function, which we assume from now on to be centered at the internuclear axis midpoint. Under this condition, the calculated angular momentum transfer is zero for a symmetric molecule like H_2. The transformation from this frame to one centered at the nuclei center of mass can be easily done. The change in angular momentum transfer $\Delta\Lambda$ when the origin is shifted by x along the internuclear axis AB involves only the perpendicular friction coefficient $F_\perp$:

$$\Delta\Lambda = xF_\perp . \tag{30}$$

Therefore, the knowledge of $F_\perp$ allows us to calculate the angular momentum transfer for a molecule like HD which is electronically symmetric but whose center of mass is not at the internuclear midpoint.

The transfer of angular momentum from the electron gas to the moving molecule can be intuitively understood using a simple classical picture. If the molecule is viewed as two atoms moving independently inside a fluid with different friction coefficients, the difference in friction gives rise to an angular momentum transfer, with respect to a fixed origin, according to the classical law

$$\Lambda = \left(\frac{d}{2}\right)[F_A(r_s) - F_B(r_s)]. \tag{31}$$

Here $F_A(r_s)$ and $F_B(r_s)$ are the friction coefficients of particles A and B when moving independently in the fluid and Λ measures the angular momentum transfer with respect to the internuclear midpoint.

The latter expression neglects the interference term in the IA approximation. It is exact when one nuclear charge tends to zero. This allows us to check the procedure of Sec. II C by calculating self-consistently the potential of a hydrogen atom in a FEG with the atom set at a distance $a=d/2$ from the origin. The latter potential has axial (not spherical) symmetry and therefore requires the procedure of Sec. II C to calculate Λ. The results plotted in Fig. 6 show that Λ depends linearly on a, as expected from Eq. (31). The slope of the curves in Fig. 6 ($F_H=0.254$, 0.164, and 0.098 for $r_s=2$, 3, and 4, respectively) agrees within less than 1% with the friction coefficients of H in a FEG (see Fig. 2).

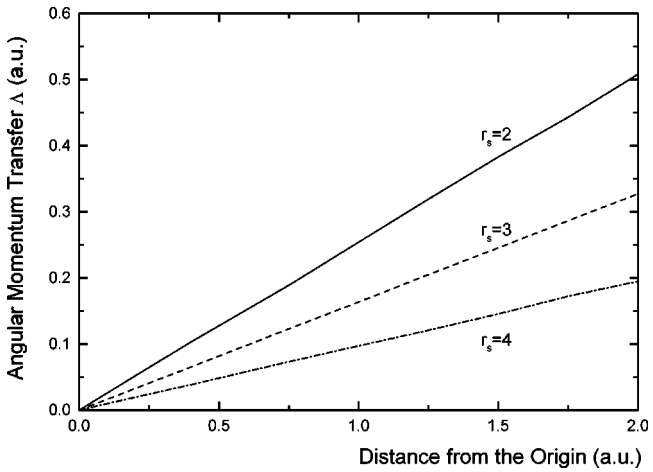

FIG. 6. Angular momentum transfer Λ for a hydrogen atom moving inside a free-electron gas, as a function of the distance from the origin of coordinates. The results are plotted for three different values of the electronic density of the medium: $r_s=2$ (solid line), $r_s=3$ (dashed line), and $r_s=4$ (dash-dotted line).

In order to estimate the importance of the electron-hole pair excitation in the rotation of the molecule, we have chosen LiH as a model system. We place the H nucleus at A and the Li nucleus at B (Fig. 1). We plot in Fig. 7 the angular momentum transfer Λ for LiH moving inside a FEG as a function of electronic density. As a reference we also plot in Fig. 7 the value of Λ calculated using the classical law of Eq. (31), with $F_{\mathrm{Li}}(r_s)$ and $F_{\mathrm{H}}(r_s)$ being the friction coefficients of Li and H moving independently inside a FEG. Figure 7 shows that the sign of Λ changes when going from low to high values of r_s, the crossing point being at $r_s \approx 2.9$. In other words, the sense of rotation switches depending on the medium electronic density. This behavior can be explained by comparison with Eq. (31) (dashed line of Fig. 7): for large values of r_s the stopping of H is larger than that of Li, but the opposite is true for small values of r_s. Our results follow roughly the same trend.

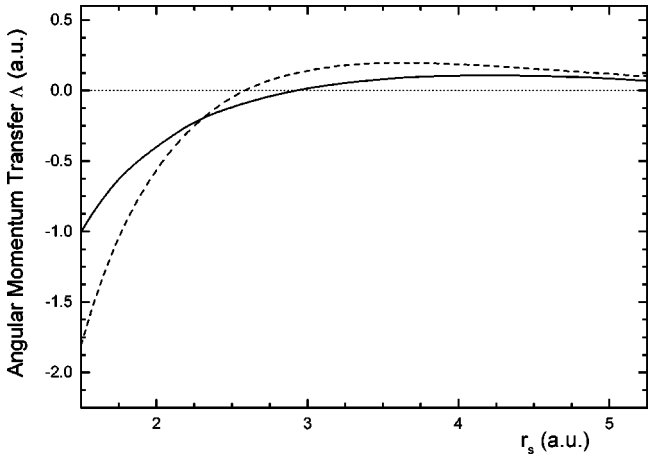

FIG. 7. Angular momentum transfer Λ for LiH moving inside a free-electron gas, as a function of the electronic density parameter r_s. The internuclear distance is the equilibrium distance in the vacuum. The solid line is the result of the full calculation and the dashed line is obtained using Eq. (31). The zero is shown with a dotted line.

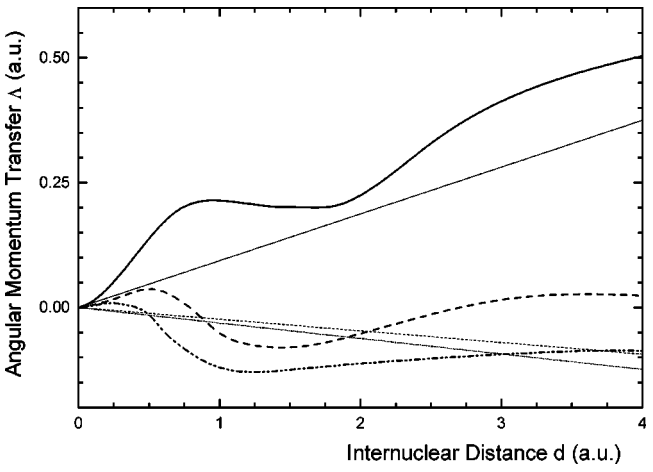

FIG. 8. Angular momentum transfer Λ for LiH moving inside a free-electron gas, as a function of the internuclear distance. The results are plotted for three different values of the electronic density of the medium: $r_s=2$ (solid line), $r_s=3$ (dashed line), and $r_s=4$ (dash-dotted line). The thick lines show the results of the full calculation and the thin straight lines are obtained using Eq. 31.

We have also calculated the transfer of angular momentum between LiH and a FEG as a function of internuclear distance. Results are plotted in Fig. 8 for three different values of r_s, along with the values obtained using Eq. (31). The results of both calculations follow a similar trend, although the classical one is, of course, unable to reproduce the oscillations created by the interference effects between the two molecular centers in the scattering of the electrons. The sense of rotation depends on electronic density as explained above. As a general rule, the absolute value of Λ increases for larger internuclear distances as expected from the classical linear dependence.

The most noticeable feature of Fig. 7 is that the magnitude of Λ ranges between -1.0 and 0.25 a.u. for the equilibrium internuclear distance. The same order of magnitude is obtained for molecules other than LiH when calculating Λ through Eq. (31), which is a reasonable estimate of the order of magnitude of the effect, as Fig. 7 shows. This means that the excitation of electron-hole pairs can play a role in modifying the rotational state of a molecule of thermal energy approaching a surface. We can roughly estimate the effect using again the local approximation to describe the surface density profile. We discard the angular dependence of $d\langle \Delta \hat{J}_y \rangle / dR$ (i.e., we consider the molecular axis parallel to the surface) and take $\Lambda = 0.1$ a.u. as a typical value since Λ varies little with density for r_s larger than 3.5 (see Fig. 7). In order to obtain the angular momentum transfer with respect to the center of mass of the molecule (which is shifted a distance $x = 3d/8$ from the internuclear midpoint towards the Li atom) Λ_{cm}, we make use of Eq. (30). The friction coefficient $F_{\perp}$ of LiH in a FEG can be calculated following the same procedure used in the preceding section for H_2, and takes values between $F_{\perp}=0.05$ a.u. (for $r_s=5$) and $F_{\perp}=0.37$ a.u. (for $r_s=2.5$). Hence, the angular momentum transfer with respect to the center of mass is the sum of two terms, both of them of the same order of magnitude. We can estimate $\Lambda_{\mathrm{cm}} \approx 0.2$ a.u. Furthermore, we consider that the typical path length over which the molecule interacts with

the electronic density of the surface is of the order of 1 a.u. This yields a value of 0.2 a.u. for the transfer of angular momentum $\langle \Delta \hat{J}_y \rangle$. In a real experiment, the latter number means that roughly 20% of the impinging molecules can be excited/deexcited due to electronic excitations in the surface. Notice that the latter estimate is independent of the molecule velocity (to first order in v) and only depends on the interaction path.

V. CONCLUSIONS

In this work we have studied the energy dissipation of a slow dimer traveling inside a free-electron gas, as well as the transfer of angular momentum to the dimer, due to the excitation of low-energy electron-hole pairs. Kohn-Sham theory allows us to describe these processes in terms of the scattering properties of one-electron orbitals in the self-consistent potential of the dimer. We are thus including nonlinear effects both in the response of the medium to the dimer and in the calculation of the scattering amplitude. We have shown in Sec. III that, both of them being important, the latter is crucial to obtain an accurate description of the energy loss for this range of velocities. The single scattering approach implicit in the independent-atom (IA) approximation is unable to describe in a proper way the scattering properties of the Fermi electrons in realistic dimer potentials. Nevertheless, IA can be used to estimate the order of magnitude of the angular momentum transfer.

Our results are relevant to the ongoing discussion on the effects of inelastic processes in the adsorption of molecules on surfaces. Electronic excitations like the ones studied modify the values of, for example, adsorption energies and activation barriers in the adsorption process. We have shown in this work that the excitation of electron-hole pairs can play a role in reducing the kinetic energy of the molecule approaching the surface, as well as in its outgoing way after desorption. For instance, we have estimated the effect to be of the order of 10% of the incident molecule kinetic energy for H_2 molecules approaching an Al surface at 100 meV. The friction coefficient calculated in Sec. III can be used as a friction force in the description of the dynamics of the molecule. The evaluation of the adsorption threshold energies from experimental data has to include the effect of these inelastic processes.

Rotational excitation of the molecule due to the creation of electron-hole pairs has been addressed as well. The nonadiabatic friction of molecules with the electronic density of a surface can provoke rotational excitation or quenching. We remark here that the transfer of angular momentum is closely related to the friction coefficient of the molecule when its velocity is perpendicular to the molecular axis. Hence, the angular momentum transfer will be different for molecules with identical electronic structure but different dynamical properties (such as H_2 and HD, for example), due to the different position of the center of mass of the molecule. In other words, an isotope effect should arise in some of the physical properties that govern the adsorption process, such as the sticking coefficient or the kinetic energy threshold for adsorption.

ACKNOWLEDGMENTS

This work was supported in part by the Director, Office of Science, Office of Basic Energy Sciences and Director, Office of Science, Office of Basic Energy Sciences, Division of Materials Sciences under U.S. Department of Energy Contract No. DE-AC03-76SF00098. R.D.M. acknowledges financial support by the Basque Government (Programa de Formación de Investigadores del Departamento de Educación, Universidades e Investigación).

[1] R. B. Gerber, Chem. Rev. **87**, 29 (1987).
[2] G. Wahnström, in *Interactions of Atoms and Molecules with Solid Surfaces*, edited by V. Bortolani, N. H. March and M. P. Tosi (Plenum Press, New York, 1990), Chap. 16.
[3] G. R. Darling and S. Holloway, Rep. Prog. Phys. **58**, 1595 (1995).
[4] A. Amirav and M. J. Cardillo, Phys. Rev. Lett. **57**, 2299 (1986).
[5] H. Nienhaus, H. S. Bergh, B. Gergen, A. Majumdar, W. H. Weinberg, and E. W. McFarland, Phys. Rev. Lett. **82**, 446 (1999); Surf. Sci. **445**, 335 (2000).
[6] B. Hellsing and M. Persson, Phys. Scr. **29**, 360 (1984).
[7] M. Head-Gordon and J. C. Tully, J. Chem. Phys. **103**, 10 137 (1995); J. T. Kindt, J. C. Tully, M. Head-Gordon, and M. A. Gómez, *ibid.* **109**, 3629 (1998).
[8] P. J. Rous, Phys. Rev. B **59**, 7719 (1999).
[9] K. Schönhammer, Phys. Rev. B **37**, 7735 (1988).
[10] A. Salin, A. Arnau, P. M. Echenique, and E. Zaremba, Phys. Rev. B **59**, 2537 (1999).
[11] P. M. Echenique, R. M. Nieminen, and R. H. Ritchie, Solid State Commun. **37**, 779 (1981).
[12] P. M. Echenique, F. Flores, and R. H. Ritchie, Solid State Phys. **43**, 229 (1990).
[13] E. Zaremba, A. Arnau, and P. M. Echenique, Nucl. Instrum. Methods Phys. Res. B **96**, 619 (1995).
[14] E. G. d'Agliano, P. Kumar, W. Schaich, and H. Suhl, Phys. Rev. B **11**, 2122 (1975).
[15] I. Nagy, A. Arnau, and P. M. Echenique, Nucl. Instrum. Methods Phys. Res. B **48**, 54 (1990).
[16] H. M. Urbassek, V. Dröge, and R. M. Nieminen, J. Phys.: Condens. Matter **5**, 3289 (1993).
[17] R. Díez Muiño, and A. Salin, Phys. Rev. B **60**, 2074 (1999).
[18] A. Messiah, *Mécanique Quantique* (Dunod, Paris, 1962), Vol. 2, Chap. XIX, p. 692, Eq. (21).
[19] C. Cohen-Tannoudji, B. Diu, and F. Laloë, *Mécanique Quantique* (Hermann, Paris, 1973), Sec. EIII.
[20] N. F. Mott and H. S. W. Massey, *The Theory of Atomic Collisions* (Clarendon, Oxford, 1965), Chap. VIII, Sec. 3.1.
[21] J. C. Eckardt, G. Lantschner, N. R. Arista, and R. A. Baragiola, J. Phys. C **11**, L851 (1978).
[22] R. Golser, Ch. Eppacher, and D. Semrad, Nucl. Instrum. Methods Phys. Res. B **67**, 69 (1992).
[23] G. Basbas and R. H. Ritchie, Phys. Rev. A **25**, 1943 (1982).
[24] N. D. Lang and W. Kohn, Phys. Rev. B **1**, 4555 (1970).
[25] H. A. Michelsen and D. J. Auerbach, J. Chem. Phys. **94**, 7502 (1991).